Permafrost thermal response to improved soil hydro-thermodynamics
in historical and scenario simulations with a modified version of the MPI-ESM

Félix Garcia-Pereira[1], **J. F. Gonzalez-Rouco**[1], **N. Meabe-Yanguas**[1], **N. J. Steinert**[2], **P. De Vrese**[3], **J. H. Jungclaus**[3], **and S. J. Lorenz**[3]

[1]**Complutense University of Madrid (UCM) and Geosciences Institute (IGEO, UCM-CSIC), Madrid, Spain** [2]CICERO, Oslo, Norway [3]Max Planck Institute for Meteorology (MPI-M), Hamburg, Germany

Corresponding author: Félix García-Pereira (felgar03@ucm.es)

Abstract

Global warming induces temperature and water availability changes in the Arctic that affect the soil moisture and ice presence, and subsequently the soil thermal structure in permafrost regions. Notwithstanding, the interaction between soil hydrology and thermodynamics is still poorly represented by most of the CMIP6 land surface models (LSMs), mainly in terms of the soil depth, vertical resolution, and coupling between hydrology and thermodynamics. This work explores the response of the Max Planck Institute Earth System Model (MPI-ESM) in historical and scenario simulations to changes in the hydrological and thermodynamic features of its LSM, JSBACH, in permafrost-affected regions. An ensemble of experiments was performed with varying soil depth and vertical resolution under three configurations of the hydro-thermodynamical coupling, which generate comparatively drier (**DRY**) or wetter (**WET**) conditions over permafrost areas compared to the reference (**REF**) configuration.

Results show that deepening JSBACH reduces the intensity of near-surface warming, reducing the deep permafrost degradation area by ca. 2 million km^2 and constraining the active layer thickness deepening by the end of the 21st century in high radiative forcing scenarios. Nevertheless, the largest impacts on permafrost extent and active layer thickness are produced by the DRY and WET settings, which yield diverging soil moisture and warming conditions during the 21st century.

1. The JSBACH-HTCp ensemble

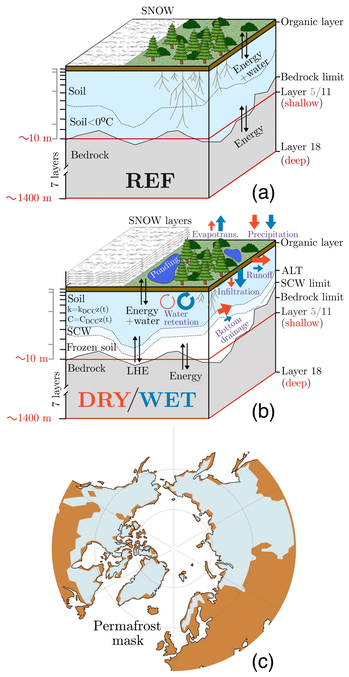

Fig. 1. HTCp thermo-hydrodynamical changes applied to JSBACH standard version (REF, a). (b) Conceptual sketch showing the features and the intensity (arrow thickness) of different thermodynamical and hydrological processes for DRY (red) and WET (blue) configurations with respect to REF. (c) Permafrost mask where the JSBACH-HTCp physics are implemented [1]. Outside the area portrayed by the permafrost mask in (c), the REF configuration of JSBACH is used.

A modified version of JSBACH3.2 (Fig. 1a, [2]) allowing for hydro-thermodynamical soil coupling in permafrost regions in fully-coupled MPI-ESM simulations [3,4] is used in this work (**JSBACH-HTCp**; Fig. 1b). These changes are active only across the areas covered by the mask shown in Fig. 1c. They consist of the inclusion of a multi-layer snow scheme, the dynamical response of soil thermal properties to hydrological changes, the allowance of water phase changes within the soil (soil ice formation), an improved representation of the organic layer, and the inclusion of a wetland scheme [3,5]. Furthermore, the JSBACH3.2 standard vertical scheme of 5 layers with a LSM depth of 9.83 m was deepened and refined near the surface. Thus, two new vertical layering schemes are introduced (Fig. 1a,b): a resolution-enhanced 11-layer scheme with a LSM depth of 9.83 m, and a deepened 18-layer scheme of 1391.48 m, which ensures the bottom layer thermal decoupling from ground surface conditions in multi-centennial timescales [6,7].

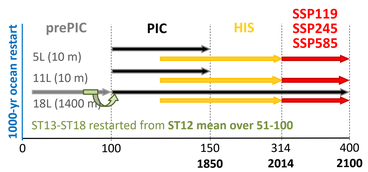

Fig. 2. Experimental setup of the MPI-ESM JSBACH-HTCp ensemble. Scheme of pre-industrial control (prePIC, grey; PIC, black), historical (HIS, yellow), and 21st century climate change Shared Socioeconomic Pathway forcing scenarios (SSP119, SSP245, and SSP585, red arrows) simulations for the three different JSBACH-HTCp configurations (DRY, WET, and REF; Fig. 1) and vertical discretizations (5, 11, and 18 layers).

The sensitivity of permafrost dynamics to changes in the standard JSBACH soil hydrology (REF, Fig. 1a) is assessed tuning some processes and parametrizations of the Arctic water-cycle, creating the WET and DRY configurations (Fig. 1b). These two configurations aim to represent two extreme hydrological states of the Arctic covering the range of uncertainty shown by CMIP6 models in future climate simulations. An ensemble of nine Pre-industrial control (**PIC**), historical (**HIS**, 1850-2014) and scenario (**SSP**, 2015-2100) simulations is conducted (Fig. 2) by combining the three configurations WET, DRY, and REF and the three LSM discretizations, with 5, 11, and 18 layers. To speed up subsurface temperature equilibrium in the vertical column for the 18-layer simulations, a prior pre-industrial control (**prePIC**) phase of 100 years is run and the subsurface temperature mean for the last 50 years at the 12th layer is used to restart temperatures at layers 13th to 18th.

2. Soil temperature variability in the JSBACH-HTCp ensemble

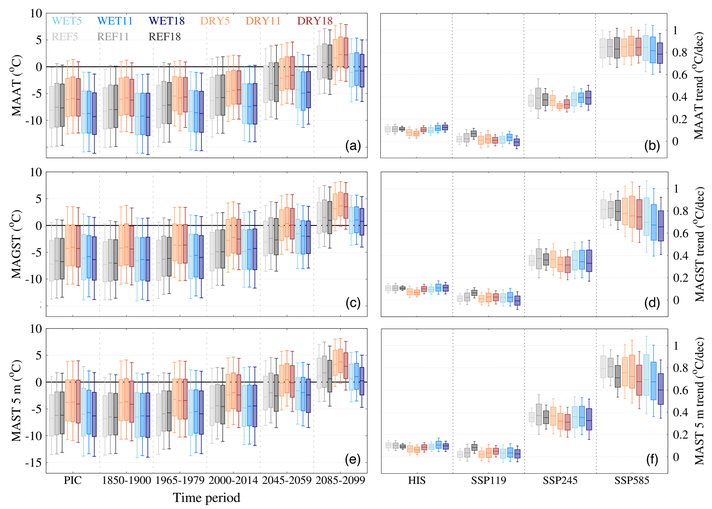

Fig. 3. Temperature variability in the JSBACH-HTCp ensemble. Mean annual air temperature (MAAT, a), ground surface temperature (MAGST, c), and soil temperature at 5 m (MAST 5 m, e) spatial boxplots, in ^{o}C, for the 9 simulations of the JSBACH-HTCp ensemble (see legend for colors and Fig. 2) in different periods. The inner tick in the boxplot marks the median value within the permafrost mask area (Fig. 1c), the bottom and top lines depict the quartiles 1 and 3, and the bottom and top whiskers percentiles 10 and 90, respectively. MAAT (b), MAGST (d), and MAST 5 m (f) spatial trend boxplots, in ^{o}C/decade, for HIS and SSP585 scenario periods are also portrayed.

The initial PIC state for MAAT, MAGST, and MAST 5 m (Fig. 3a,c,e) permafrost spatial variability does not remarkably change in the 19th and 20th centuries. WET simulations are on average 2 ^{o}C colder than DRY, and similar to REF. As warming in the 21st century progresses, REF temperature increases more than WET (0.8 vs. 0.7 ^{o}C/decade for SSP585), which produces a spatial REF-WET offset of up to 1.5 ^{o}C by the end of the century, and a REF spatial median temperature close to DRY. MAAT spatial values are always colder than MAGST and MAST 5 m for DRY and WET, which might be driven by an improved representation of snow insulation in winter [8]. The effect of deepening JSBACH is remarkable for MAST 5 m, the 18-layer being colder and the trends lower than for 5 and 11-layer simulations.

3. Active layer thickness (ALT) response to HTCp changes

ALT spatial values are the smallest for WET (Fig. 4a). This is due to the relative colder regional temperatures compared to DRY and REF simulations (Fig. 3). However, REF spatial median ALT is ca. 1 m greater than DRY up to the first quarter of the 21st century, despite showing colder MAAT, MAGST, and MAST 5 m (Fig. 3a,c,e). Fig. 4b,c further shows ALT for REF is greater than 75 for DRY for ca. 70 (60) % of the points in the 1850-1900 (2000-2014) period. This overall overestimation of REF ALT with temperature is most likely due to the fact that the standard JSBACH does not include freezing-thawing processes, neglecting the "counterbalance" zero-curtain effect [9] in summer.

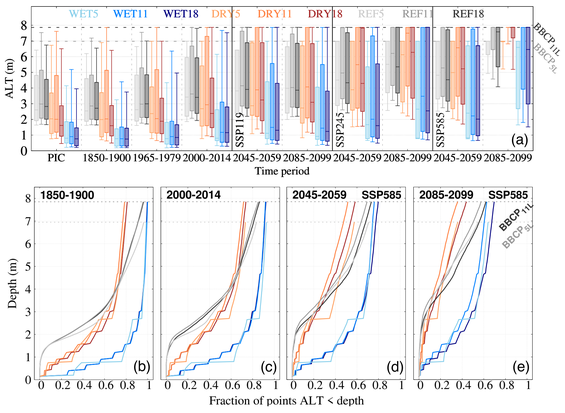

Fig. 4. (a) Active layer thickness spatial distribution (ALT, m) for the JSBACH-HTCp ensemble in different periods (see Fig. 3). (b-e) Fraction of points within the JSBACH-HTCp permafrost mask with an ALT in summer smaller than the indicated depth in the y-axis for different periods. For every plot, dark (light) gray dashed line indicates the LSM depth for the (5) 11-layer configuration.

Moreover, deepening JSBACH reduces ALT thickening with warming for the three HTCp configurations, preventing that ca. a 10 % of the permafrost points are completely thawed by 2085-2099 (Fig. 4e).

4. Permafrost extent (PE): JSBACH-HTCp vs. CMIP6 ensemble

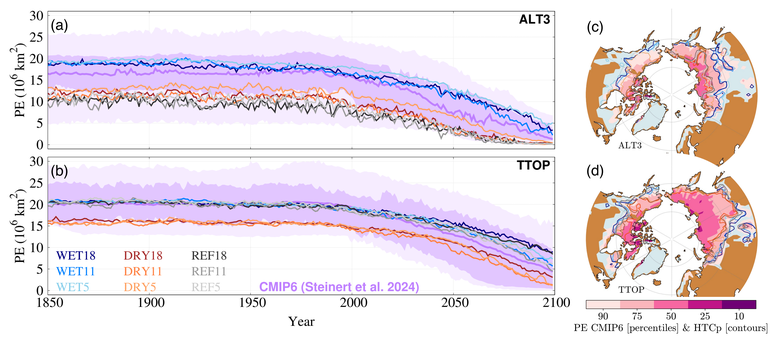

Fig. 5. PE time evolution in the JSBACH-HTCp and CMIP6 ensembles. (Left) PE (in millions of km^2) according to ALT3 (a) and TTOP (b) permafrost definitions. Lines of different colors (see legend within panel b) indicate the different members of the ensemble, and (light) purple shading portray the CMIP6 interquartilic (P90-P10) range for PE estimates stemming from CMIP6 models given by [10]. (Right) PE maps for JSBACH-HTCp ensemble members (contour lines) and CMIP6 ensemble (filled contours) in 2045-2059 for ALT3 (c) and TTOP (d).

PE is compared in terms of the permafrost area where ALT is above a soil depth of 3 m (ALT3; Fig. 5a,c) and soil temperature at the top of the permafrost is greater than 0 ^{o}C (TTOP; Fig. 5b,d). In both cases, pre-industrial and 20th century WET PE is close to CMIP6 median, DRY lying close to Q1. REF renders smaller PE values than DRY for ALT3, and greater and closer to WET for TTOP, which might be linked to the lack of soil water phase changes. As SSP5 warming intensifies, PE loss is more intense for shallow (5 and 11) than for deep (18-layer) simulations for TTOP, suggesting a stronger deep-permafrost degradation.

Acknowledgements

We acknowledge the financial support of the Spanish Ministry of Science to GreatModelS (RTI2018-102305-B-C21) and SMILEME (PID2021-126696OB-C21) projects, and funding FGP Ph.D.'s contract (PRE2019-090694). We would also thank the Deutsches Klimarechenzentrum (DKRZ) for the resources its Scientific Steering Committee (WLA) granted to run the JSBACH-HTCp ensemble under project ID bm1026.

References

[1] Hugelius, G., et al. (2014), **BG**, DOI: 10.5194/bg-11-6573-2014.
[2] Reick, C. H., et al. (2021), **MPI-M**, DOI: 10.17617/2.3279802.
[3] de Vrese, P., and Brovkin, V. (2021), **Nat. Comm.**, DOI: 10.1038/s41467-021-23010-5.
[4] de Vrese, P., et al. (2023), **TC**, DOI: 10.5194/tc-17-2095-2023.
[5] Ekici, A., et al. (2014), **GMD**, DOI: 10.5194/gmd-7-631-2014.
[6] González-Rouco, J. F., et al. (2021), **JHM**, DOI: 10.1175/JHM-D-21-0024.1.
[7] Melo-Aguilar, C., et al. (2018), **CP**, DOI: 10.5194/cp-14-1583-2018.
[8] Steinert, N. J., et al. (2021), **GRL**, DOI: 10.1029/2021GL094273.
[9] Outcalt, S., et al. (1990), **WRR**, DOI: 10.1029/WR026i007p01509.
[10] Steinert, N. J., et al. (2024), **ERL**, DOI: 10.1088/1748-9326/ad10d7.